Demonstration of surface plasmons in metal island films and the effect of the surrounding medium—An undergraduate experiment

P. Orfanides, T. F. Buckner, M. C. Buncick, F. Meriaudeau, and T. L. Ferrell

Citation: American Journal of Physics **68**, 936 (2000); doi: 10.1119/1.1285859
View online: http://dx.doi.org/10.1119/1.1285859
View Table of Contents: http://aapt.scitation.org/toc/ajp/68/10
Published by the American Association of Physics Teachers

Demonstration of surface plasmons in metal island films and the effect of the surrounding medium—An undergraduate experiment

P. Orfanides, T. F. Buckner, and M. C. Buncick
Department of Physics, The University of Memphis, Memphis, Tennessee 38152

F. Meriaudeau
LE21, 12 rue de la fonderie, 71200 Le Creusot, France

T. L. Ferrell
Oak Ridge National Laboratory, Oak Ridge, Tennessee 37831

(Received 10 September 1999; accepted 16 November 1999)

We present a demonstration of the surface plasmon phenomenon as it occurs in thin metal island films. The metal films are deposited on glass microscope slides. The effect of the surface plasmon resonance may be observed visually on the slide without further apparatus. Heating the film changes the shape of the islands and therefore the resonant frequency of the surface plasmon and changes the color of the film. Placing the film in a dielectric medium changes the resonance condition for the surface plasmon again and changes the color again. We show this by coating the slides with commercially available liquids with different indices of refraction. We present a theoretical model that assumes the islands are oblate spheroids. There are enough details given so that the equations can be programed and the theoretical optical absorbance can be reproduced. We also present a modification to the theory so that the shift in resonant frequency can be calculated when the spheroids are immersed in the index fluids. We describe our apparatus for making thin films and our optical spectrometer system. We then present optical absorbance measurements of thin films of both Ag and Au in air and in two liquids with different indices of refraction.

I. INTRODUCTION

Surface plasmons were discovered in 1957[1] and since then there has been considerable study of the fundamental properties of plasmons and their applications. For applications, a wide variety of work has been done in seemingly disparate areas. For example, studies have been made of surface plasmon contributions to surface-enhanced Raman scattering,[2] surface interactions with photoemission,[3] and optical-grating characterization.[4] Surface plasmon resonance has been used to produce a wide variety of optical sensors. A surface plasmon can be generated by the interaction of an electron-rich surface, such as that of a metal, with a charged particle or with a photon. It is a collective, quantized oscillation of the conduction electrons near the surface of the metal or semiconductor.

Surface plasmons can be generated in continuous thin films (30–50 nm) by using configurations in which light is incident on the film from a medium with an index of refraction greater than 1. A common configuration to accomplish this is the Kretschmann configuration.[5] In this configuration, shown in Fig. 1, the light is incident on the film through the prism and at an angle greater than the critical angle. The evanescent wave interacts with the film and generates the surface plasmon. The surface plasmon is detected by carefully adjusting the angle of incidence. When the surface plasmon angle (θ_{sp}) is reached, the reflected intensity is dramatically quenched as the energy is transferred to the film.

Surface plasmons can be effectively generated in metal or semiconductor particles when the spatial dimensions of the particle are smaller than half the wavelength of the light incident on the particle. It has been known for some time that the condensation of evaporated metal onto a substrate does not produce continuous, microscopically uniform films.[6] For films less than 20 nm thick, the materials are deposited at nucleation points producing electrically isolated islands. This phenomenon is attributed to high surface mobility. There has been extensive investigation of the optical properties of metal island films[7–12] with several theories applied to model the optical response of these films. The surface plasmon for island films can be generated by direct interaction with incident light and does not require the prism configuration of the continuous thin films. The surface plasmon can be detected by simply measuring the optical transmittance of an island film.

For both thin films and island films, the resonance condition which generates the surface plasmon is very sensitive to the optical properties of the dielectric medium in contact with the film. This phenomenon has been extensively exploited to develop a tremendous variety of sensors and remains a very intense area of research. A chemically sensitive layer applied to the film has allowed the development of sensors such as immunoassay,[13] gas,[14] and liquid.[15] Surface plasmon resonance has emerged as a powerful tool in biosensing.[16] Its ability to probe dynamic surface processes in real time and *in situ* without biomarkers is almost without peer. Traditionally, the Kretschmann configuration with continuous films is used in these sensors. This configuration is relatively large and expensive and difficult to implement for remote sensing applications. However, several surface plasmon sensors have been developed that are essentially miniature versions of the Kretschmann configuration. One such version, developed by Texas Instruments,[17] is a chip with an LED array light source and a photodiode array along with signal analysis hardware. The surface of the chip is covered with a flattopped glassy material that acts as the prism. The flattop is metal coated and light is totally reflected from the lower side of this surface. The light couples into the metal

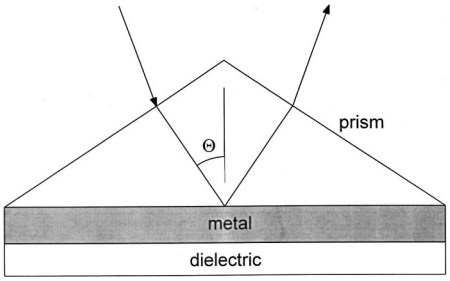

Fig. 1. A configuration for generating surface plasmons in thin continuous films in each. The light is coupled into the film by the evanescent wave from totally internally reflected light.

and generates plasmons. A sensing medium is attached to the metal. This device is now being marketed as a hand-held chemical sensor. Plasmon sensors using continuous films have also been developed on optical fibers.[18,19] Because the light in a fiber is confined by total internal reflection, the fiber functionally replaces the prism. The metal film is deposited on the fiber surface and a sensing layer is applied to the film. The optical transmittance of the fiber is used to sense the presence of the analyete. A commercial version of this sensor is available from Pharmacia (Uppsala, Sweden). A fiber optic sensor using island films has been developed using two different configurations. The sensitivity has been demonstrated and applications are under development.[20,21]

Several experiments demonstrating surface plasmons in continuous thin films suitable for undergraduate participation have been reported over the years in this Journal.[22–24] They all use the Kretschmann configuration, which requires a metal-coated prism or bringing a prism into intimate contact with a metal-coated surface. This requires development of a suitable holder to coat the prism or some clamping system to force the prism surface into sufficient contact with the film. The surface plasmon may be observed by rotating the prism and measuring the reflectance as a function of angle of incidence. The prism must be rotated precisely using a suitable rotation platform as the entire effect of surface plasmon resonance occurs within one degree of rotation of the angle of incidence. Alternatively, the resonance may be observed using a spectrometer to scan through wavelengths keeping the angle of incidence constant.

We present a demonstration of the surface plasmon phenomenon as it occurs in thin metal island films. This experiment is simplified over the continuous film version in several ways. First, our metal films are deposited on glass microscope slides. The effect of the surface plasmon resonance may be observed visually on the slide without further apparatus because the color of the slide is not the characteristic color of the metal that forms the film. Heating the film changes the shape of the islands and, therefore, the resonant frequency of the surface plasmon, and the color of the film. Placing the film in a dielectric medium also changes the resonance condition for the surface plasmon and changes the color again. We show this by coating the slides with commercially available liquids with different indices of refraction. We present a theoretical model that assumes the islands are oblate spheroids. There are enough details given so that the equations can be programed and the theoretical optical absorbance can be reproduced. We also present a modification to the theory so that the shift in resonant frequency can be calculated when the spheroids are immersed in the index fluids. We describe our apparatus for making thin films and our optical spectrometer system. We then present optical absorbance measurements of thin films of both Ag and Au in air and in two liquids with different indices of refraction.

II. THEORETICAL DEVELOPMENT

A theory to describe the absorbance spectra of oblate spheroids was developed by Kennerly *et al.*[8] following a formalism developed by Ritchie *et al.*[25] We present a summary of the theory here and show the equations required to calculate the optical absorbance. Two assumptions in our analysis are the following. First, that the particles are much smaller than the wavelength of light and therefore we may apply nonretarded electrodynamics (the dipole approximation) and, second, that the particles are noninteracting. Laplace's equation in oblate spheroidal coordinates is

$$\nabla^2\Phi=\frac{1}{a^2(\eta^2+\mu^2)}\left[\frac{\partial}{\partial\eta}\left((1+\eta^2)\frac{\partial\Phi}{\partial\eta}\right)+\frac{\partial}{\partial\eta}\left((1-\mu^2)\frac{\partial\Phi}{\partial\mu}\right)+\frac{\eta^2+\mu^2}{(1+\eta^2)(1-\mu^2)}\frac{\partial^2\Phi}{\partial\phi^2}\right]=0. \tag{1}$$

Here η is a coordinate that, held constant ($\eta=\eta_0$), describes the surface of a spheroid, and μ is a coordinate that, held constant ($\mu=\mu_0$), describes a hyperboloid which intersects the surface of the spheroid orthogonally. The focal length is a and θ is the angle between the z axis and the asymptote of the hyperboloids. Laplace's equation is solved to obtain the electric potential inside and outside the spheroid. The potential are

$$\Phi_{\text{inside}}=\sum_{l=0}\sum_{m=0}\sum_{p=\pm1}A_{lmp}Q_{lm}(i\eta)P_{lm}(i\eta)Y_{lmp}(\theta,\phi), \tag{2}$$

$$\Phi_{\text{outside}}=\sum_{l=0}\sum_{m=0}\sum_{p=\pm1}A_{lmp}Q_{lm}(i\eta)P_{lm}(i\eta)Y_{lmp}(\theta,\phi), \tag{3}$$

where $Q_{lm}(i\eta)$ and $P_{lm}(i\eta)$ are the Legendre functions of imaginary argument, Y_{lmp} are the real spherical harmonics, and the position angles θ and ϕ are the same as those in spherical coordinates and as described above. The incident electric field induces a surface charge density at the surface of the spheroid that may be calculated from the difference in the electric field inside and outside the spheroid. These electric fields may be obtained by taking the negative gradient of the potentials. We assume an idealized charge density that is zero everywhere except at the surface. So the surface charge density is related to the volume charge density by a delta function and a scale factor

$$\rho=\frac{\sigma\delta(\eta-\eta_0)}{h_{\eta_0}}, \tag{4}$$

where h_η is the scale factor and is given by

$$h_{\eta_0}=a\sqrt{\frac{\eta_0^2+\mu^2}{\eta_0^2+1}}. \tag{5}$$

The volume charge density may be integrated over the volume of the spheroid to give the dipole moment. The polarizabilities α_x, α_y, and α_z of the spheroid along the three Cartesian axes follow from the dipole moment. They are

$$\alpha_x = \frac{2a^3(1+\eta_0^2)^{1/2}[\epsilon(\omega)-1]}{3Q_{11}(i\eta_0)[\epsilon(\omega)-\epsilon_{11}(i\eta_0)]}, \tag{6}$$

$$\alpha_y = \frac{2a^3(1+\eta_0^2)^{1/2}[\epsilon(\omega)-1]}{3Q_{11}(i\eta_0)[\epsilon(\omega)-\epsilon_{11}(i\eta_0)]}, \tag{7}$$

$$\alpha_z = \frac{-a^3\eta_0[\epsilon(\omega)-1]}{3Q_{10}(i\eta_0)[\epsilon(\omega)-\epsilon_{10}(i\eta_0)]}. \tag{8}$$

Here η_0 is called the shape parameter and represents the surface of the spheroid. The range of η_0 is 0 to ∞, where $\eta_0=0$ is a straight line between the focal points of the ellipse and $\eta_0=\infty$ is a circle of infinite radius. For a spheroid, η_0 is related to the minor to major axis ratio (R) by

$$\eta_0 = \frac{R}{\sqrt{(1-R^2)}}. \tag{9}$$

The ϵ_{lm} are the dispersion relations for the spheroid and they are

$$\epsilon_{11} = 1 - \frac{2}{\eta_0(1+\eta_0^2)\cot^{-1}\eta_0 - \eta_0^2} \tag{10}$$

and

$$\epsilon_{10} = 1 + \frac{1}{(1+\eta_0^2)(\cot^{-1}\eta_0 - 1)}. \tag{11}$$

$\epsilon(\omega)$ is the complex dielectric response function for the metal that forms the spheroid. An extensive compilation of optical constants of elements and compounds may be found in a multivolume set of books edited by Palik.[26] The Legendre polynomials are

$$Q_{10}(i\eta) = \eta\cot^{-1}\eta - 1, \tag{12}$$

$$Q_{11}(i\eta) = (1+\eta^2)\left[\cot^{-1}\eta - \frac{\eta}{1+\eta^2}\right]. \tag{13}$$

From the expressions for induced dipole moment, the scattered fields at large distances from the spheroid may be calculated and combined with the incident field to find the total power dissipated by the spheroid. This leads to the following expressions for the total cross section:

$$|\sigma_{\text{total}}|_s = \frac{4\pi\omega}{c}\,\text{Im}(\alpha_x), \tag{14}$$

$$|\sigma_{\text{total}}|_p = \frac{4\pi\omega}{c}\,\text{Im}(\alpha_y\cos^2\theta + \alpha_z\sin^2\theta), \tag{15}$$

where θ is the angle of incidence of the incoming light. The subscripts s and p denote light polarized perpendicular and parallel to the plane of incidence, respectively. The absorbance is defined as

$$A = \log_{10}\left(\frac{1}{1-N\sigma}\right), \tag{16}$$

where N is the density of particles and is determined by microscopy.

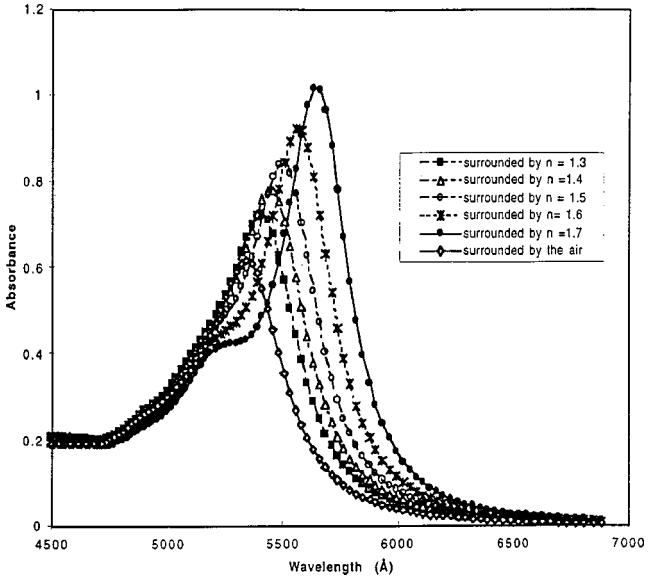

Fig. 2. Calculated absorbance as a function of wavelength for gold islands on a quartz slide and surrounded by fluids with different indices of refraction. The angle of incidence is 0° and the shape parameter is 0.7. This gives a peak in air at 540 nm.

If the metal particles are surrounded by a dielectric, the resonance frequency of the surface plasmon can be shifted. We can approximate this effect for the spheroids by using the analogy of a thin uniform dielectric film in contact with a dielectric material. The details have been reported previously[27] and we report a summary here so that the calculation may be reproduced by the reader. We calculate modified versions of ϵ_{11} and ϵ_{10} in the same manner as with a continuous film giving new resonance conditions and strengths. Here we assume that the particles are lying on a substrate and are represented by a metal of thickness a and with dielectric function $\epsilon_0(\omega)$. The metal is coated by a dielectric material with dielectric function $\epsilon_a(\omega)$. The dispersion relation is then

$$\epsilon^2(\omega) + \epsilon(\omega)(\epsilon_a(\omega)+\epsilon_0(\omega))\coth(Ka) + \epsilon_a(\omega)\epsilon_0(\omega) = 0, \tag{17}$$

where K is the wave vector of the surface plasmon. By analogy with the continuous thin film dispersion relation, Eq. (17) can also be written as

$$\epsilon^2(\omega) - \epsilon(\omega)(\epsilon_{11}+\epsilon_{10})\left[\frac{\epsilon_a(\omega)+\epsilon_0(\omega)}{2}\right] + \epsilon_a(\omega)\epsilon_0(\omega)\epsilon_{11}\epsilon_{10} = 0. \tag{18}$$

This quadratic equation can be solved for new values of ϵ_{11} and ϵ_{10} that can be substituted into the polarizability expressions and from these a new absorbance curve may be generated. An example of the results of the theoretical optical absorbance is shown in Fig. 2. Here we have plotted the optical absorbance of an Au film with the shape parameter η_0 set to 0.7 that corresponds to an absorption peak in air with a maximum absorbance at 535 nm. The plot shows the effect of immersing the particles in dielectric media with different indices of refraction. The results are similar for Ag films except that the peak positions are shifted about 100 nm toward the blue end of the spectrum.

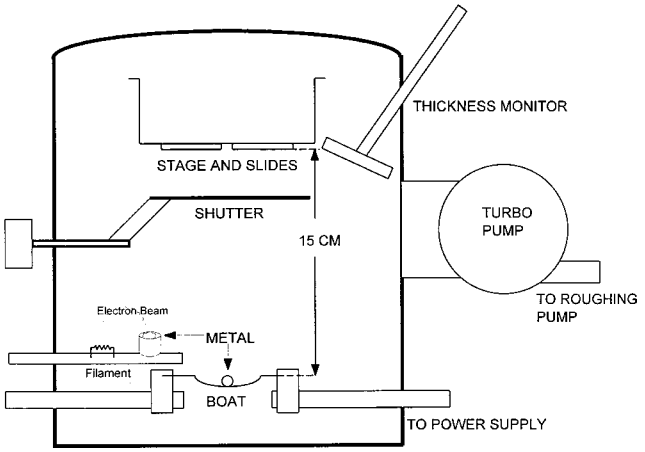

Fig. 3. A schematic of the deposition system used to produce the metal films. The system has both an e-beam and a thermal deposition system in the chamber and is pumped by a turbo pump.

III. EXPERIMENT

A. Apparatus

In this section we will describe the procedure and equipment used in the deposition and data acquisition. Film depositions are made in a metal bell jar vacuum chamber that contains both an e-beam and a thermal vapor deposition system. A diagram of the deposition system is shown in Fig. 3. This vacuum system is pumped by a 300 ℓ/s turbo pump backed by a direct-drive rotary oil roughing pump. A molecular sieve filter is used in the foreline to minimize backstreaming. Substrates are held in the upper part of the chamber on the bottom side of a deposition stage. The thickness and deposition rate of the deposited material are determined by a quartz crystal thickness monitor. A rotatable shutter separates the substrate from the deposition boat or the e-beam hearth until the proper deposition rate is established.

The apparatus used for the optical measurements is a low-cost system but the measurements can be performed in any UV–visible spectrophotometer. The optical components are mounted on an optical bench and a diagram of the optical system appears in Fig. 4. A quartz–halogen 21 V–150 W lamp is powered by a Lambda regulated power supply. The light from the lamp passes through an iris open to about 0.5 cm, where it then passes through the sample. A UV transmitting filter from ESCO Products, Inc.[28] follows, to enhance the wavelengths of 370 to 500 nm. The light is collected by a 25-mm-diam fiber optic collimator from Sigma-Netics, Inc.[29] and is transmitted to an Ocean Optics, Inc. model SD2000 fiber optic spectrometer.[30] The spectrometer is interfaced to a Pentium® PC with acquisition software supplied by the spectrometer manufacturer.

B. Sample preparation

Films were deposited on glass microscope slides cleaned with a 5-min acetone wash in an ultrasonic cleaner followed by a 5-min methyl alcohol wash in the ultrasonic cleaner. The slides are then blown dry and mounted on the deposition stage. The metal used is 99.999% Ag or Au in 1- to 3-mm chunks.[31]

Depositions can be made with either the e-beam deposition system or with the thermal vapor deposition apparatus. Films deposited by either system give identical results. Depositions are usually made at base pressures between 5 and 8×10^{-7} Torr. Film thicknesses for this experiment were 60 Å deposited at a rate of 1 Å/s. Samples that were heated to change the particle shape were heated in a quartz tube lined furnace that was held at 250 °C for the Ag samples and 400 °C for the Au samples. Each sample was heated for 1 min. An atomic force microscope (AFM) image of an unheated Au film is shown in Fig. 5(a) and the Au film after heating is shown in Fig. 5(b). The heating causes the surface tension of the metal to draw the islands from a flat pancake shape into a shape similar to a door knob. This change in shape causes a shift in the resonance frequency of the plasmon. Immersing the particles in a dielectric medium produces a depolarizing effect because of image charge formation in the dielectric. This depolarization also causes a shift in the resonance frequency of the surface plasmon.

The microscope slides were cut into four equal pieces for data acquisition. Two of them are heated and the others are left unmodified. The samples are placed in a holder that keeps them vertical in front of the iris. A cover slide is placed on top of the metallized surface of each of the slides. When measurements are made using index matching fluid, the fluid is applied to the edges of the ''glass sandwich,'' where capillary action spreads the fluid evenly over the internal surfaces. Optical absorbance curves were obtained for both heated and unheated samples in air, in $n=1.5$ fluid, and in $n=1.75$ fluid. Data were acquired for the same Ag or Au films before and after the insertion of the index fluid. Two bare glass slides are used as a reference for samples with no index fluid. Using two slides with fluid as a reference helped compensate for some thin film effects of the thin fluid layer but these effects were not eliminated for the $n=1.75$ fluid. The optical absorbance of this fluid increases dramatically at wavelengths below about 380 nm. The index fluids used were obtained from R. P. Cargille Laboratories, Inc.[32] and

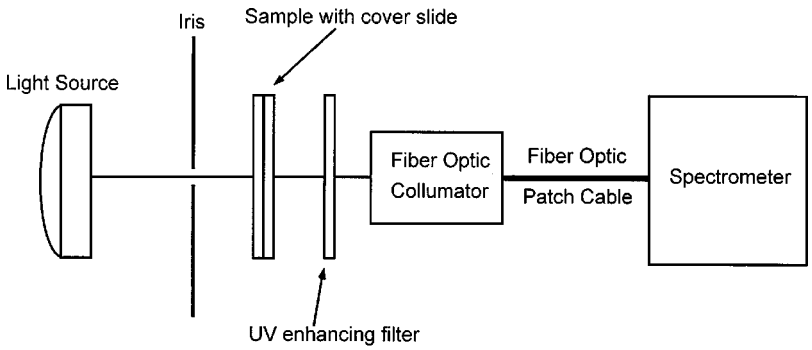

Fig. 4. The optical system used to measure the optical absorbance of the metal island films.

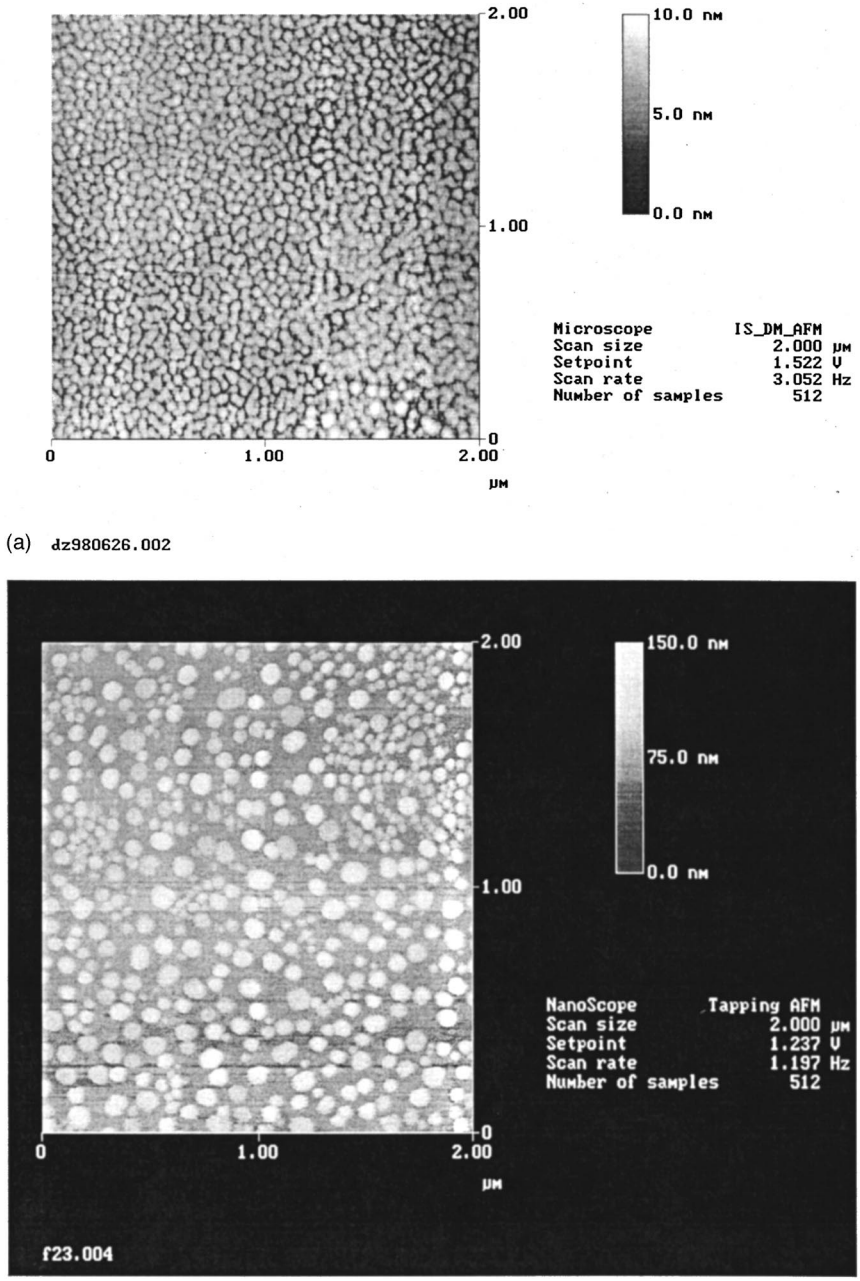

Fig. 5. (a) A 2 μm$\times$2 μm atomic force microscope (AFM) image of a 60-Å gold sample evaporated onto a glass slide. (b) The same film after heating to 400 °C for 1 min.

are 1.500 ± 0.002, series A, and index liquid 1.750 ± 0.005, series M. These index fluids are nonabsorbing in the visible and so do not contribute to the optical absorbance of the gold and silver films.

IV. RESULTS

A. Silver

A photo of a typical Ag film is shown in Fig. 6. We show an as-deposited unheated film on the left, a film heated to 250 °C on the right, and with $n = 1.75$ fluid surrounding the particles on part of the heated film. A cover slide has been placed on the fluid to make a uniform film. At the bottom, Fig. 6 also shows a slide with the same fluid and a cover slide to show that the fluid is transparent in the visible. The 60-Å silver film looks purple before heating. After 1 min of heating at 250 °C the film turns yellow. With the 1.75 index fluid added, the covered part of the slide changes color, again becoming purple, having almost the same color it had before heating. With the index fluid of 1.50 (not shown), the Ag film turned pink. These results are easily reproducible.

The optical absorbance of Ag as a function of wavelength for an unheated film and heated films in air, $n = 1.5$ fluid, and $n = 1.75$ fluid is shown in Fig. 7. The unheated samples have a broad absorbance with a peak around 550 nm with minimum absorbance at about 400 nm. This absorbance minimum corresponds to the blue color of the unheated films. After heating, with the samples in air, the absorbance peak narrows considerably with a maximum absorbance of 0.5 at a wavelength of 425 nm. With the narrowing of the absorbance peak, the film removes the blue part of the visible, leaving the yellow color when viewed in transmission. When submerged in the index fluid of 1.500, the peak shifts to 500 nm, with an absorbance of 0.7. This shift removes more of

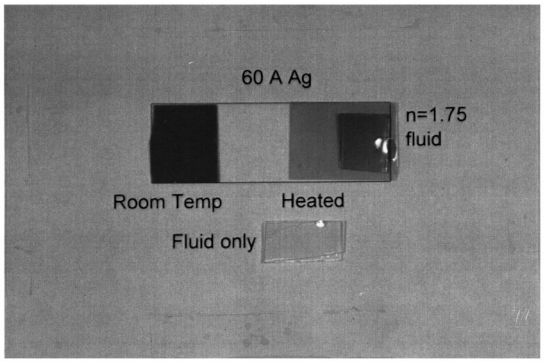

Fig. 6. A photo of a 60-Å Ag film. The slide on the left-hand side is the as-deposited island film and is purple in color. The slide on the right-hand side is the film after heating to 250 °C for 1 min. The left half is the film in air and is yellow and the right half is the film covered with $n=1.75$ fluid and a cover slide. The left half is yellow and the film covered with the $n=1.75$ is purple. The slide at the bottom is the fluid on a bare slide with a cover slide showing that the fluid has no color.

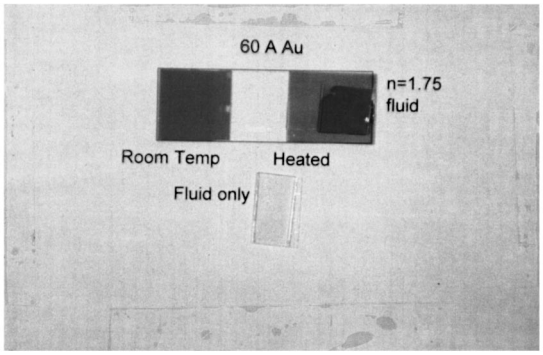

Fig. 8. A photo of a 60-Å Au film. The slide on the left-hand side is the as-deposited island film. The slide on the right-hand is the film after heating to 400 °C for 1 min. The left half is the film in air and the right half is the film covered with $n=1.75$ fluid and a cover slide. The unheated film is blue–green and the heated film in air is reddish pink. The heated film in the $n=1.75$ fluid is blue. The slide at the bottom is the fluid on a bare slide with a cover slide showing that the fluid has no color.

the visible spectrum, leaving the transmitted color in the red. Finally, with the 1.750 index fluid, the peak occurs at a wavelength of 600 nm, reaching an absorbance of 0.65. The blue part of the spectrum is now transmitted and the film appears blue. These absorbance results are in agreement with the results of the model presented earlier. A comparison of Figs. 7 and Fig. 2 shows that the absorbance increases and shifts toward the red end of the spectrum as the index of the surrounding medium increases.

B. Gold

The procedure for the preparation and data acquisition of the gold films is identical to that for the silver films except that, since Au has a higher melting point, the 60-Å-thick Au films were heated at 400 °C for 1 min. Figure 8 shows an Au film in the same configuration as the Ag film with an unheated slide on the left and heated one on the right. Part of the heated film is covered with a cover slide and has the $n=1.75$ fluid on the particles. As with the Ag film, the index fluid is applied to a sample with a cover slide to make the fluid uniform thickness. The unheated Au films appear blue–green in transmittance and turn reddish pink after heating. After the 1.500 index fluid was inserted, the films appeared yellow, and with the 1.750 fluid the film appears blue. Color photographs of these Ag and Au films may be viewed on the web at www.people.memphis.edu/~physics/mcb/mbuncick.html.

The optical absorbance of Au as a function of wavelength for an unheated film and heated films in air, $n=1.5$ fluid, and $n=1.75$ fluid is shown in Fig. 9. The gold samples in air have a broad absorbance with a peak around 800 nm. The film appears blue–green, because the minimum absorbance is at about 525 nm and the film transmits well from 525 to 400 nm. In the heated samples, the absorbance peak is again narrowed significantly and is a maximum at approximately 560 nm at about 0.30 absorbance units. The minimum absorbance is at the red end of the spectrum and also transmits well between about 500 and 400 nm. Thus the film appears reddish pink due to the combination of red and blue. With the 1.500 index fluid the peak absorbance shifts to 625 nm at an absorbance of about 0.38 with a minimum absorbance at

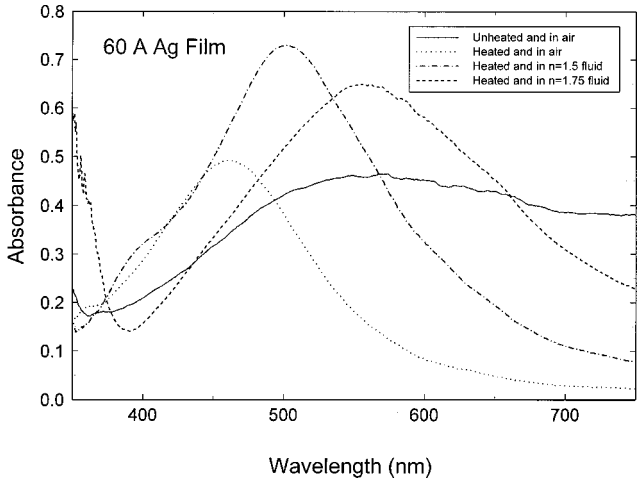

Fig. 7. The optical absorbance as a function of wavelength for a 60-Å Ag film. The plot shows absorbance curves for an unheated film, a heated film in air, and the heated film in $n=1.5$ and $n=1.75$ fluid.

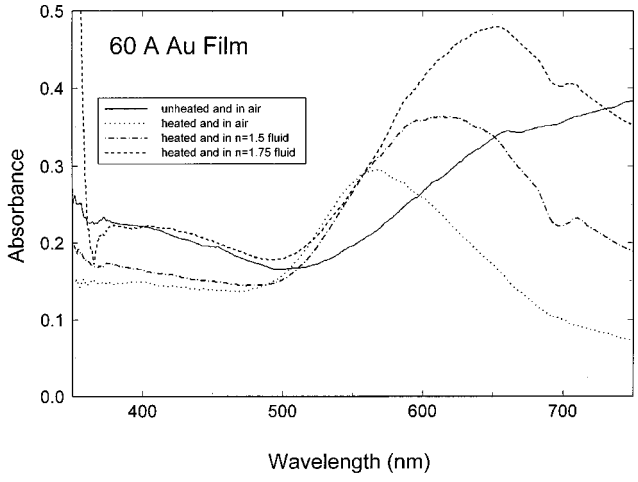

Fig. 9. The optical absorbance as a function of wavelength for a 60-Å Au film. The plot shows absorbance curves for an unheated film, a heated film in air, and the heated film in $n=1.5$ and $n=1.75$ fluid.

about 500 nm. The transmitted red plus the transmitted green give the yellow color of the film. Finally, with the 1.750 index fluid, the absorbance peak was shifted by another 50 nm, to 675 nm, and reached an absorbance of about 0.48. Now the red is removed from the transmitted light, leaving the green and blue part of the spectrum and the film appears blue. Again the characteristic redshift and increase in absorbance occurs with increasing index of the surrounding medium as predicted by the model.

V. CONCLUSION

We have demonstrated how metal island films can be used to show the effect of surface plasmon resonance on the optical properties of the films. The color of the film changes as the shape of the islands changes and after the film is immersed in a dielectric medium. This property has been exploited to make optical sensors. The films may be prepared in a common thin film deposition chamber. The generation of these films along with a duplication of the theory could be used as a project in an advanced lab or as part of an optics course. The dramatic changes in the color of the film can be demonstrated on an overhead projector for a more general audience.

ACKNOWLEDGMENT

We would like to express our gratitude to Dr. Patrick Oden of Oak Ridge National Laboratory for providing us with the AFM images.

[1]R. H. Ritchie, ''Plasma losses by fast electrons in thin films,'' Phys. Rev. **106**, 874–881 (1957).
[2]T. L. Ferrell, ''Surface-enhanced Raman scattering in Ag-pyride sols,'' Phys. Rev. B **25**, 2930–2932 (1982).
[3]T. A. Callcott and E. T. Arakawa, ''Volume and surface photoemission processes from plasmon resonance fields,'' Phys. Rev. B **11**, 2750–2758 (1975).
[4]R. H. Ritchie, E. T. Arakawa, J. J. Cowan, and R. N. Hamm, ''Surface-plasmon resonance effect in grating diffraction,'' Phys. Rev. Lett. **21**, 1530–1533 (1968).
[5]C. R. Lawrence and N. J. Geddes, in *Handbook of Biosensors and Electronic Noses*, edited by E. Kress-Rodgers (CRC Press, Boca Raton, FL, 1997), p. 149.
[6]J. Eastermann, ''Über die Straker dünner Silberniedschläge,'' Z. Phys. Chem., Stoechiom. Verwandtschaftch. **106**, 403–406 (1923).
[7]J. W. Little, T. L. Ferrell, T. A. Callcott, and E. T. Arakawa, ''Radiative decay of surface plasmons on oblate spheroids,'' Phys. Rev. B **26**, 5953–5956 (1982).
[8]S. W. Kennerly, J. W. Little, R. J. Warmack, and T. L. Ferrell, ''Optical properties of heated Ag films,'' Phys. Rev. B **29**, 2926–2929 (1984).
[9]R. J. Warmack and S. L. Humphrey, ''Observation of two surface plasmon modes on gold particles,'' Phys. Rev. B **34**, 2246–2252 (1986).
[10]M. C. Buncick, R. J. Warmack, and T. L. Ferrell, ''Optical absorbance of silver ellipsoidal particles,'' J. Opt. Soc. Am. B **4**, 927–933 (1987).
[11]M. J. Bloemer, T. L. Ferrell, M. C. Buncick, and R. J. Warmack, ''Optical properties of submicrometer-size silver needles,'' Phys. Rev. B **37**, 8015–8021 (1988).
[12]M. J. Bloemer, T. L. Ferrell, M. C. Buncick, and R. J. Warmack, ''Surface electromagnetic modes in prolate spheroids of gold, aluminum, and copper,'' J. Opt. Soc. Am. B **5**, 2552–2559 (1988).
[13]P. B. Daniels, J. K. Deacon, M. J. Eddowes, and D. Pedley, ''Surface plasmon resonance applied to immunosensing,'' Sens. Actuators **15**, 11–18 (1988).
[14]B. Liedberg, C. Nylander, and I. Lundström, ''Surface plasmon resonance for gas detection and biosensing,'' Sens. Actuators **4**, 299–304 (1983).
[15]R. Matsubaru, S. Kawata, and S. Minami, ''Optical chemical sensor based on surface plasmon measurement,'' Appl. Opt. **27**, 1160–1163 (1988).
[16]J. Davies, ''Surface plasmon resonance—The technique and its applications to biomaterial processes,'' Nanobiology **3**, 5–16 (1994).
[17]Information on this sensor can be found at: http://www.ti.com/spr/
[18]R. C. Jorgenson and S. S. Yee, ''A fiber optic sensor based on surface plasmon resonance,'' Sens. Actuators B **12**, 213–220 (1993).
[19]W. J. H. Bender, R. E. Dessy, M. S. Miller, and R. O. Claus, ''Feasibility of a chemical microsensor based on surface plasmon resonance on fiber optics modified by multilayer vapor deposition,'' Anal. Chem. **66**, 963–970 (1994).
[20]F. Meriaudeau, T. Downey, A. Passian, A. Wig, M. C. Buncick, and T. L. Ferrell, ''Fiber optic sensor based on surface plasmon resonance,'' Sens. Actuators B **54**, 106–117 (1999).
[21]F. Meriaudeau, A. Wig, A. Passian, T. Downey, M. C. Buncick, and T. L. Ferrell, ''Gold Island fiber optic sensor,'' Sens. Actuators B (submitted).
[22]H. J. Simon, D. E. Mitchell, and J. G. Watson, ''Surface plasmons in silver films—A novel undergraduate experiment,'' Am. J. Phys. **43**, 630–636 (1975).
[23]J. D. Swalen, J. G. Gordon, II, M. R. Philpott, A. Brillante, I. Pockrand, and R. Santo, ''Plasmon surface polariton dispersion by direct optical observation,'' Am. J. Phys. **48**, 669–672 (1980).
[24]A. S. Barker, ''An optical demonstration of surface plasmons on gold,'' Am. J. Phys. **42**, 1123–1126 (1974).
[25]R. H. Ritchie, J. C. Ashley, and T. L. Ferrell, in *Electromagnetic Surface Modes*, edited by A. D. Boardman (Wiley, New York, 1982), Chap. 3.
[26]*Handbook of Optical Constants of Solids*, edited by E. D. Palik (Academic, San Diego, 1998), Vols. I–III are optical constants of elements and compounds.
[27]P. Royer, J. P. Goudonnet, R. J. Warmack, and T. L. Ferrell, ''Substrate effects on surface-plasmon spectra in metal-island films,'' Phys. Rev. B **35**, 3753–3759 (1987).
[28]ESCO Products, Inc., 171 Oak Ridge Road, Oak Ridge, NJ 07438.
[29]Sigma-Netics, Inc., 1 Washington Ave., Fairfield, NJ 07004.
[30]Ocean Optics, Inc., 380 Main St., Dunedin, FL 34698.
[31]Cerac, Inc., P.O. Box 1178, Milwaukee, WI 53201-1178.
[32]R. P. Cargille Labs, Inc., 55 Commerce Rd., Cedar Grove, NJ 07009.

BRONZE COINAGE

Teachers are often urged to show enthusiasm for their subjects. Did you ever have to listen to a really enthusiastic specialist holding forth on something that you did not know and did not want to know anything about, say the bronze coinage of Poldavia in the twelfth century or ''the doctrine of the enclitic *De*''? Well, then.

Ralph P. Boas, Jr., ''Can We Make Mathematics Intelligible?,'' in *Lion Hunting & Other Mathematical Pursuits*, edited by Gerald L. Alexanderson and Dale H. Mugler (Mathematical Association of America, Washington, 1995), p. 235.